Articles

Contribution from the Division of Chemical and Physical Sciences, Deakin University, Waurn Ponds 3217, Victoria, Australia, and Chemistry Department, Faculty of Science, Australian National University, Canberra 2601, ACT, Australia

Novel Synthesis of Reduced Mixed-Valence Molybdenum and Tungsten Complexes by Electrochemical Oxidation of the Seven-Coordinate Complexes $MX(S_2)(R_2dtc)_2$ (M = Mo, X = O; M = W, X = O, S; R = Alkyl; dtc = Dithiocarbamate)

A. M. Bond,*[1] J. A. Broomhead,*[2] and A. F. Hollenkamp[1]

Received August 26, 1987

The electrochemical oxidation and reduction of a series of seven-coordinate complexes $M^{VI}X(S_2)(R_2dtc)_2$ (M = Mo, X = O; M = W, X = O, S; R = alkyl; dtc = dithiocarbamate) have been studied at both platinum and mercury electrodes in a range of organic solvents. At platinum electrodes a single irreversible oxidation process is observed at around 1.0 V vs Ag/AgCl. The potential is largely independent of the metal and the dithiocarbamate R group and, in the case of tungsten, whether X is oxygen or sulfur, which is consistent with a ligand-based oxidation process initially involving the disulfide (S_2^{2-}) group. Data at mercury electrodes support this conclusion although the oxidation process occurs at a potential different from that observed at platinum electrodes. Surprisingly, the ultimate metal-containing product of oxidation (controlled-potential electrolysis (1.5 ± 0.1 faraday mol^{-1}) or chemical oxidation with $NOPF_6$) is a mixed-valence molybdenum(V)-molybdenum(IV) dimer in which the metal has been reduced. For $MoO(S_2)(R_2dtc)_2$ (R = Me, Et), oxidation yields isolable yellow (R = Me) or orange (R = Et) $[Mo^{IV}Mo^{V}O_2(R_2dtc)_4]PF_6$, which has been characterized by elemental analysis, conductivity measurements, and IR and EPR spectroscopy. This compound can be reduced to form the molybdenum(IV) species, $MoO(R_2dtc)_2$, which can in turn be oxidized back to form the mixed-valence dimer. Reduction of $MX(S_2)(R_2dtc)_2$ at platinum electrodes is an irreversible two-electron process at room temperature with slow scan rates (100 mV s^{-1}) but becomes a chemically reversible one-electron step at -70 °C or with fast scan rate cyclic voltammetry (50 V s^{-1}) at 20 °C. The initially formed $[M^{V}X(S_2)(R_2dtc)_2]^-$ anion is inherently unstable and decreases its coordination number while undergoing further reduction. The reduction potentials, in contrast to the oxidation potentials, follow established trends for metal-based processes with $WO(S_2)(R_2dtc)_2$ being more difficult to reduce than $MoO(S_2)(R_2dtc)_2$ while replacement of oxygen with sulfur in the former facilitates reduction. Reduction at mercury electrodes is again substantially different from that at platinum electrodes. Isolation of the products of reduction proved difficult except for $WS(S_2)(R_2dtc)_2$ in which case reduction with cobaltocene, $CoCp_2$, yields deep red $[CoCp_2][W^{IV}S(S_2)R_2dtc]$.

Recently the novel seven-coordinate complexes $WX(S_2)(R_2dtc)_2$ (X = O, S; R = alkyl; dtc = dithiocarbamate) have been synthesised[3,4]. These complexes are structurally similar to the previously reported oxomolybdenum complex $MoO(S_2)(n\text{-}Pr_2dtc)_2$[5] and a structural representation is given in I. The pentagonal-

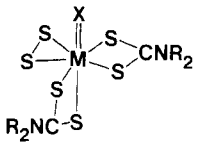

I

bipyramidal structure is typical of that found for seven-coordinate oxomolybdenum(VI) complexes.[6-8] Crystallographic data for $WO(S_2)(Et_2dtc)_2$[3] show distorted-pentagonal-bipyramidal geometry about the metal center with a terminal oxo group and a η^2-disulfido ligand in a mutually triangular arrangement. The metal-sulfur (dithiocarbamate) bond trans to the terminal chalcogen is longer than the rest.

There are very few reports describing the redox properties of seven-coordinate molybdenum(VI) and tungsten(VI) complexes. Chen et al.[9] showed significant differences in the ease of reduction with regard to the metal present for the species $M^{VI}OY_2(Et_2dtc)_2$ (M = Mo, W; Y = Cl, Br). This class of molybdenum complex is susceptible to chemical reduction with loss of halide or transfer of oxygen whereas the tungsten analogues display a relative inertness. The generation of stable metal(V) species for molybdenum (i.e. $MoOY(Et_2dtc)_2$, but not for tungsten, is also noteworthy.

In view of the close relationship to $MoOY_2(Et_2dtc)_2$, it is readily predicted that reduction of $MoO(S_2)(R_2dtc)_2$ should be possible under electrochemical conditions. Replacement of halide with the disulfide group offers the prospect of electrochemical oxidation away from the metal center. After oxidation substantial rearrangement and/or internal redox processes could occur and lead to novel molybdenum and tungsten compounds. Chemical oxidation of Mo-S and W-S systems can lead to changes in both the metal and sulfur oxidation states.[10] The number and proximity of sulfur atoms in the coordination sphere may be significant factors in their electrochemical oxidation. Stiefel et al. have suggested that short S-S distances for adjacent ligands may lead to direct involvement of the ligand in electron-transfer reactions.[10,11]

In the present work, detailed electrochemical studies on a series of $MX(S_2)(R_2dtc)_2$ complexes have been undertaken to establish the importance of the (S_2^{2-}) group in electron-transfer properties in both oxidation and reduction reactions. The oxidation reactions are particularly novel since they lead to isolation of a paramagnetic

(1) Deakin University.
(2) Australian National University.
(3) Broomhead, J. A.; Enemark, J. H.; Hammer, B.; Ortega, R. B.; Pienkoswki, W. *Aust. J Chem.* **1987**, *40*, 381.
(4) Pan, W.-H.; Halbert, T. R.; Hutchings, L. L.; Stiefel, E. I. *J. Chem. Soc., Chem. Commun.* **1985**, 927.
(5) Dirand-Colin, J.; Schappacher, M.; Ricard, L.; Weiss, R. *Proceedings of the 2nd International Conference on the Chemistry and Uses of Molybdenum*; Mitchell, P. C. H., Seaman, A., Eds.; Climax Molybdenum: London, 1976; p 46.
(6) Drew, M. G. *Prog. Inorg. Chem.* **1977**, *23*, 67.
(7) Melník, P.; Sharrock, P. *Coord. Chem. Rev.* **1985**, *65*, 49.
(8) Stiefel, E. *Prog. Inorg. Chem.* **1977**, *22*, 1.
(9) Chen, G. J.-J.; McDonald, J. W.; Newton, W. E. *Inorg. Chim. Acta* **1980**, *41*, 49.
(10) Harmer, M. A.; Halbert, T. R.; Pan, W.-H.; Coyle, C. L.; Cohen, S. A.; Stiefel, E. I. *Polyhedron* **1986**, *5*, 341 and references cited therein.
(11) Stiefel, E. I.; Miller, K. F.; Bruce, A. E.; Corbin, J. L.; Berg, J. M.; Hodgson, K. O. *J. Am. Chem. Soc.* **1980**, *102*, 3624.

0020-1669/88/1327-0978$01.50/0

Table I. Infrared and ^{1}H NMR Data for $WX(S_2)(R_2dtc)_2$ Complexes (X = O, S)

complex	infrared freq,[a] cm^{-1}			^{1}H NMR shift[b]	
	ν(S—S)[c]	ν(M=X)[c]	ν(CN)[c]	$\delta(CH_2)$[d]	$\delta(CH_3)$[d]
$WO(S_2)(Et_2dtc)_2$	550 s	940 vs	1510 s	q:[e] 3.50, 3.80 3.84, 3.88	t:[f] 1.14, 1.39 1.40, 1.42
$WS(S_2)(Et_2dtc)_2$	548 s	495 s	1520 s	q:[e] 3.42, 3.77 3.84, 3.87	t:[f] 1.11, 1.38 1.41[g]
$WO(S_2)(Me_2dtc)_2$	548 s	930 vs	1525 s		
$WS(S_2)(Me_2dtc)_2$	542 m	495 s	1530 vs		s:[f] 3.02, 3.36 3.43, 3.47
$WS(S_2)(i\text{-}Pr_2dtc)_2$[h]	542 m	494 m	1490 vs		
$WS(S_2)(Pyrrdtc)_2$[i]	540 m	490 vs	1490 vs, br		

[a] Recorded as CsI or KCl disks. [b] Recorded as $CDCl_3$ solutions versus $Si(CH_3)_4$. [c] Key: vs, very strong; s, strong; m, medium; br, broad. [d] Key: s, singlet; t, triplet; q, quartet. [e] Integrates for 2 H. [f] Integrates for 3 H except *g*. [g] Two overlapping signals; integrates for 6 H. [h] *i*-Pr = isopropyl. [i] Pyrrdtc = pyrrolidine-*N*-carbodithioate.

mixed-valence M(V)/M(IV) complex. That is, oxidation of metal(VI) complexes may lead to synthesis of reduced molybdenum and tungsten species as an alternative to reduction, which is more obviously and naturally directed toward this goal. The results compliment those available for related dithiocarbamate complexes such as $Mo^{IV}O(Et_2dtc)_2$,[12] $Mo^{VI}O_2(Et_2dtc)_2$[12,13] $Mo^{VI}S_2(Et_2dtc)_2$,[12] $Mo^{IV}(Et_2dtc)_4$,[14,15] $[W^V(Et_2dtc)_4]Br$.[14]

Experimental Section

Materials. All solvents used were of analytical or HPLC grade and were dried with alumina. The supporting electrolytes tetraethyl- and tetrabutylammonium perchlorate, Et_4NClO_4 and Bu_4NClO_4, as well as tetrabutylammonium hexafluorophosphate, Bu_4NPF_6, were obtained from South Western Analytical (Austin, TX) and were dried under vacuum at 70 °C to remove water.

Syntheses. (i) $WO(S_2)(R_2dtc)_2$ and $WS(S_2)(R_2dtc)_2$. These compounds were first prepared recently via oxidation of $W(CO)_3(R_2dtc)_2$ complexes[3] while the latter series has also been prepared by reaction of WS_4^- with $R_2NC(S)S\text{–}SC(S)NR_2$ (tetraalkylthiuram disulfide).[4] For this study, methods employing $W(CO)_3(R_2dtc)_2$ precursors were used, and an example for the case of R = ethyl (Et) is given. A stirred solution of $W(CO)_3(Et_2dtc)_2$ in CH_2Cl_2 (1.4 g in 80 mL) was purged with SO_2 for 1 h. During this time, the original orange color changed to red-brown and a brown solid deposited. This was filtered off and the filtrate evaporated to dryness. The residue was dissolved in a small volume of CH_2Cl_2 and chromatographed (under N_2) on a silica gel column using CH_2Cl_2/hexane (4:1) as the eluent. Green, red-brown, and yellow fractions were eluted in that order. Each was dried over anhydrous Na_2SO_4, filtered, and evaporated to dryness. The species produced were green $WS(S_2)(Et_2dtc)_2$ (13%) and red-brown $WO(S_2)(Et_2dtc)_2$ (35%) with the yellow product being $W_2O_2S_2(Et_2dtc)_2$ in very low yield.

Alternatively, stirring $W(CO)_3(Et_2dtc)_2$ (0.8 g) in CH_2Cl_2 (40 mL) with S (0.4 g) under N_2 for 1.5 h gave a persulfido complex $WS(S_2)(Et_2dtc)_2$ in 50% yield. Spectroscopic data (IR and ^{1}H NMR) for some of the complexes are given in Table I. Proton NMR studies are consistent with the retention of seven coordinate geometry in solution.

(ii) $MoO(S_2)(R_2dtc)_2$. Complexes in this series were synthesized according to literature methods[5] using $Mo(CO)_3(R_2dtc)_2$ as the starting material.

(iii) $[Mo_2O_2(Me_2dtc)_4](PF_6)$. To a stirred solution of $MoO(S_2)(Me_2dtc)_2$ (21.6 mg/0.05 mmol) in 30 mL of dichloromethane was added equimolar $NOPF_6$ (8.8 mg) as a solid. Within 30 min the deep blue color was discharged to give a yellow solution. Addition of diethyl ether precipitated a yellow solid, which when recrystallized from benzene/dichloromethane gave a fluffy yellow product. Anal. Calcd for $[Mo_2O_2(Me_2dtc)_4](PF_6)$: C, 16.96; H, 2.85; N, 6.59; S, 30.2; O, 4.1. Found: C, 17.43; H, 2.66; N, 6.55; S, 29.5; O, 4.1. (Analysis by AMDEL—Australian Microanalysis Service (Fishermen's Bend, Victoria, Australia)).

(iv) $[Mo_2O_2(Et_2dtc)_4](PF_6)$. To a stirred solution of $MoO(S_2)(Et_2dtc)_2$ (24.5 mg/0.05 mmol) in 30 mL of dichloromethane was added $NOPF_6$ (8.8 mg) as a solid. The deep blue/green color was replaced by orange within 30 min and a crude product isolated by addition of diethyl ether. Recrystallization from dichloromethane/ether yielded orange needles.

Instrumentation. Electrochemistry. (i) Slow scan rate voltammetric measurements were made with a Princeton Applied Research Corp. (Princeton, NJ) PAR Model 174A polarographic analyzer. Polarograms were recorded with a dropping mercury working electrode while cyclic voltammograms at platinum electrodes were obtained with a small polished disk electrode. For experiments with a rotating platinum electrode a Metrohm Model 628-10 drive unit and Model 628-50 electrode assembly were used. A platinum wire served as the auxiliary electrode while the reference electrode consisted of Ag/AgCl (saturated LiCl in ethanol) separated from the test solution by a salt bridge containing the appropriate solvent. For fast scan rate measurements the instrument employed was a Bioanalytical Systems (West Lafayette, IN) BAS Model 100 electrochemical analyzer. The type and configuration of electrodes was the same as that described above except that a platinum wire was employed as a quasi-reference electrode. The potential of the $[(C_5H_5)_2Fe/(C_5H_5)_2Fe^+]$ redox couple versus the Ag/AgCl reference electrode was measured frequently by oxidation of 5×10^{-4} M $(C_5H_5)_2Fe$ to provide an internal check on the stability of the reference electrode. Electrochemical measurements were made in solvent containing 0.1 M of supporting electrolyte.

(ii) Controlled-potential electrolysis experiments were performed at either a mercury pool or a platinum-gauze working electrode with a PAR Model 173 potentiostat/galvanostat in conjunction with a PAR Model 179 digital coulometer. The platinum-gauze auxiliary electrode was isolated from the test solution via a salt bridge, and the reference electrode was the same as that used for voltammetry.

Infrared Spectroscopy. Infrared spectra of solid samples were recorded in Nujol mulls on KBr disks by using a Perkin-Elmer 457 grating infrared spectrophotometer over a frequency range of 300–4000 cm^{-1} with polystyrene as the calibrant.

Conductivity Measurements. These were made in a conventional cell with a Radiometer (Copenhagen) CDM80 conductivity meter in conjunction with a Radiometer CDC104 conductivity electrode.

Electron Paramagnetic Resonance. EPR data were obtained on a Varian E-9 X-band spectrometer employing 100-kHz modulation. The reference compound was DPPH, and spectra were recorded in dichloromethane solutions at 22 °C.

Mass Spectrometry. Electron-impact positive ion mass spectra were obtained on a Finnigan 3200 series quadrupole instrument. Samples were introduced via a solids probe at 200–350 °C under the following conditions: electron energy, 30–70 eV; filament emission current, 0.5 mA; collector voltage, 34.8 V; electron multiplier voltage, 1.6 V; pressure, $(3\text{–}5) \times 10^{-6}$ Torr.

Results and Discussion

Oxidation Studies. (i) Oxidation Processes of $MoO(S_2)(R_2dtc)_2$ at Platinum Electrodes. Figure Ia shows the electrochemical oxidation (cyclic voltammetry) at a platinum electrode for $MoO(S_2)(Et_2dtc)_2$ in dichloromethane at 20 °C. A single well-defined chemically irreversible response is observed at moderately positive potentials of around 1 V vs Ag/AgCl. At a rotating platinum disk electrode (Figure 1b) the limiting current per unit concentration for the oxidation is consistent with a 1.5 ± 0.2 electron electron-transfer process (by comparison with the known two-electron reduction process as described later). The oxidation peak potential (E_p^{ox}) does not show the organic substituent effect[16,17] normally associated with the dithiocarbamate

(12) De Hayes, L. J.; Faulkner, H. C.; Doub, W. H., Jr.; Sawyer, D. T. *Inorg. Chem.* **1975**, *14*, 2110.
(13) Lamache, M.; Sanbuichi, F. *Electrochim. Acta* **1981**, *26*, 1525.
(14) Nieuwpoort, A.; Varadi, Z. B. *Inorg. Nucl. Chem. Lett.* **1974**, *10*, 801.
(15) Smith, D. A.; Schultz, F. A. *Inorg. Chem.* **1982**, *21*, 3035.
(16) Chant, R.; Hendrickson, A. R.; Martin, R. L.; Rohde, N. M. *Aust. J. Chem.* **1973**, *26*, 2533.

Table II. Voltammetric Data for the Oxidation of $MX(S_2)(R_2dtc)_2$ Complexes (M = Mo, X = O; M = W, X = O, S) in Dichloromethane (0.1 M Bu_4NClO_4) at 20 °C

	Pt electrode cyclic voltammetry[a]		Hg electrode	
			polarography[b]	cyclic voltammetry[c]
compd[d]	E_p^{ox},[f] V	E_p^{red},[e,f] V	$E_{1/2}$,[f] V	E_p^{ox},[f] V
$MoO(S_2)(Me_2dtc)_2$	1.06	0.33	0.55	0.54
$MoO(S_2)(Et_2dtc)_2$	1.04	0.28	0.53	0.56
$MoO(S_2)(Bz_2dtc)_2$[g]	1.14	0.18	0.57	0.64
$MoO(S_2)(c\text{-}Hx_2dtc)_2$[h]	1.05	0.02	0.57	0.60
$MoO(S_2)(Pyrrdtc)_2$	1.06	0.24	0.52	0.59
$WS(S_2)(Bz_2dtc)_2$[g]	1.02	0.45	0.70	0.79
$WS(S_2)(Pyrrdtc)_2$	0.96	0.48	0.59	0.69
$WO(S_2)(Et_2dtc)_2$	1.09	0.04	*i*	0.62
sulfur	*j*	*j*	0.49	0.54

[a] Platinum disk electrode, scan rate = 500 mV s^{-1}. [b] Dropping mercury electrode, drop time = 0.5 s. [c] Slowly growing dropping mercury electrode, scan rate = 500 mV s^{-1}. [d] Solution concentration = 1.0×10^{-4} M. [e] This process corresponds to the reduction of an oxidation product of the primary oxidation process and is not part of a chemically reversible redox couple. [f] Potential vs Ag/AgCl (saturated LiCl–CH_3CH_2OH). $E_{1/2}$-$[(C_5H_5)_2Fe/(C_5H_5)_2Fe^+]$ = 0.500 V vs Ag/AgCl (saturated LiCl–CH_3CH_2OH). [g] Bz = benzyl. [h] c-Hx = cyclohexyl. [i] A number of complex processes observed. [j] No oxidation response observed.

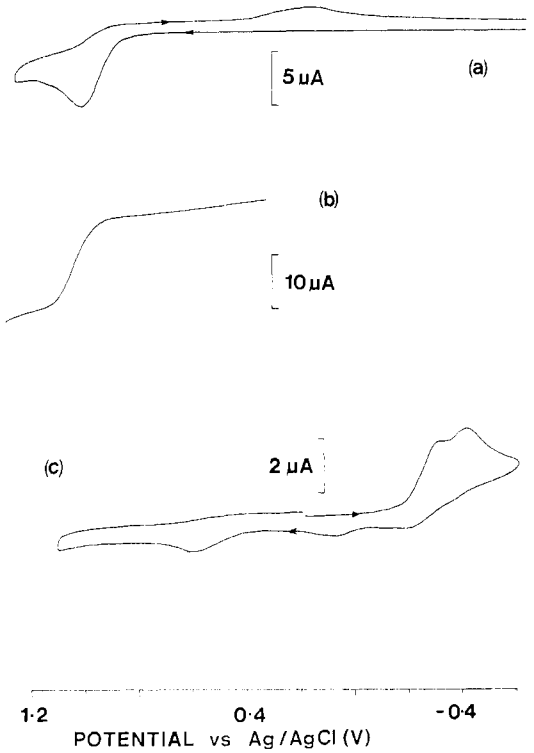

Figure 1. Voltammograms at a platinum electrode: (a) 2.5×10^{-4} M $MoO(S_2)(Et_2dtc)_2$, oxidative cyclic voltammogram (scan rate = 500 mV s^{-1}); (b) 1.0×10^{-4} M $MoO(S_2)(Et_2dtc)_2$, oxidative rotating disk electrode voltammogram (rotation rate = 2000 rev min^{-1}); (c) 1.6×10^{-4} M $[Mo_2O_2(Et_2dtc)_4](PF_6)$, reductive cyclic voltammogram (scan rate = 500 mV s^{-1}). All solutions are CH_2Cl_2 (0.1 M Bu_4NClO_4) at 20 °C.

ligand. The oxidation process remains irreversible in the chemical sense at temperatures down to −70 °C and with scan rates of 50 V s^{-1}. A reduction process is observed on the reverse (reductive) scan of cyclic voltammograms at potentials (peak potentials for reduction denoted E_p^{red}) well removed from the oxidation process. The exact position of this response depends on the R group of the dithiocarbamate ligand. This process has some similarity to that observed on the reverse scans of the oxidative cyclic voltammogram for tetraethylthiuram disulfide (Et_4tds) under the same conditions. With Et_4tds, a very broad oxidation process is evident, at a potential similar to that for $MoO(S_2)(Et_2dtc)_2$, with a reduction process (also broad) centered at +0.4 V vs Ag/AgCl being observed on the reverse scan. The data for oxidation of $MoO(S_2)(R_2dtc)_2$, which are summarized in Table II, indicate that

Table III. Conductivity Data for Acetone Solutions of $[Mo_2O_2(Et_2dtc)_4]PF_6$ and Bu_4NPF_6 at 20 °C

	Λ_M, Ω^{-1} cm^2 mol^{-1}	
concn, M	$[Mo_2O_2(Et_2dtc)_4]PF_6$	Bu_4NPF_6
2.0×10^{-3}	186	159
4.0×10^{-4}	208	183
8.0×10^{-5}	222	227
1.6×10^{-5}	244	267

ligand-based electrochemical oxidation is occurring. The lack of the expected dithiocarbamate subsituent effect is indicative of the initial electron transfer taking place at the disulfide group.

Oxidative controlled-potential electrolysis of $MoO(S_2)(R_2dtc)_2$ complexes at a platinum electrode in dichloromethane at a potential of 1.15 V vs Ag/AgCl yield bright yellow solutions after the passage of 1.5 ± 0.1 faraday/mol of complex. Cyclic voltammograms at a platinum electrode after electrolysis exhibit a number of reduction processes. A major reduction process is observed at −0.3 V vs Ag/AgCl. The reduction processes at around −1 V vs Ag/AgCl are associated with the presence of elemental sulfur and oxidized dithiocarbamate products. Elemental sulfur binds strongly to the platinum surface and was also detected as the S_8 moiety, on the working electrode after electrolysis (mass spectrometric identification).

The major molybdenum-containing product of electrolysis may be isolated as a yellow to orange solid from the electrolysis cell. Figure 1c shows a reductive cyclic voltammogram at a platinum electrode for a dichloromethane solution of the isolated oxidation product for the case of R = ethyl. A broad reduction process, consisting of two incompletely resolved processes, is observed at around −0.4 V. The oxidation process at +0.6 V shown in Figure 1c, which is present in the reverse (oxidative) scan of this cyclic voltammogram, originates from a product of the reduction processes at −0.35 V. An additional peak is seen on the oxidative scan, at +0.08 V, which corresponds to the oxidation of free diethyldithiocarbamate ligand.

The isolated product of oxidation is not formed on the time scale of cyclic voltammetry. That is the processes at −0.35 V are not observed on the reverse scan of the cyclic voltammogram in Figure 1a. Elemental analysis (see Experimental Section) of the product isolated by oxidation of $MoO(S_2)(R_2dtc)_2$ using the chemical oxidant $NOPF_6$ yields an empirical formula $[Mo_2O_2(R_2dtc)_4]PF_6$. The ionic nature of this compound has been verified by conductivity measurements in acetone (Table III). Data indicate that at low concentrations the compound $[Mo_2O_2(Et_2dtc)_4](PF_6)$ behaves similarly to Bu_4NPF_6, a known 1:1 electrolyte. At concentrations above 1×10^{-4} M, however, molar conductance for the molybdenum complex significantly exceeds that for the latter. According to Geary[18] the higher values (197 Ω^{-1} cm^2 mol^{-1} at 1

(17) Bond, A. M.; Martin, R. L. *Coord. Chem. Rev.* **1984**, *54*, 23.

(18) Geary, W. J. *Coord. Chem. Rev.* **1971**, *7*, 81.

Table IV. Infrared Data for $[Mo_2O_2(R_2dtc)_4]PF_6$, $Mo_2O_3(R_2dtc)_4$, and NaR_2dtc

	IR,[a] cm^{-1}					
	$[Mo_2O_2(R_2dtc)_4]PF_6$		$Mo_2O_3(R_2dtc)_4$		NaR_2dtc	
assignt	R = Me	R = Et	R = Me[b]	R = Et[c]	R = Me	R = Et[c]
ν(C=N$^+$)	1578 s	1530 s		1500 s	1485 s	1515 s
ν(C=S)	1050 w	1080 s		1070 w	1045 w	1060 m
ν(CSS)	983 m	1000 m		970 m	965 vs	985 s
ν(Mo=O)	934 m	940 s	938 s	930 s		
ν(P—F)	848 vs	840 vs				
ν(Mo—O—Mo)[d]	688 w, 678 w	780 m, 375 m	758 w	750 s		
δ(F—P—F)	560 m	557 s				
ν(Mo—O—Mo)[e]		490 w, 470 w	435 m	470 w		
ν(Mo—S)	375 w	372 s	370 m	370 w		

[a] Recorded as KBr disks; s = strong, m = medium, and w = weak. [b] Taken from ref 21. [c] Taken from ref 13. [d] Asymmetric mode. [e] Symmetric mode.

$\times 10^{-3}$ M) approach those for a 2:1 electrolyte suggesting that dimerization of $[Mo_2O_2(Et_2dtc)_4](PF_6)$ occurs at higher concentrations. This idea is also suggested by the electrochemical data since $[Mo_2O_2(Et_2dtc)_4](PF_6)$ gives two incompletely resolved reduction peaks (Figure 1c) separated by ca. 80 mV. The ratio of these processes is dependent on both concentration and temperature. However, the magnitude (overall and relative) of the oxidation processes on the reverse scans of cyclic voltammograms are independent of the ratio of the two reductive components.

Further confirmation of the formulation of the product as $[Mo_2O_2(R_2dtc)_4]PF_6$ was obtained by bulk reductive electrolysis. Controlled-potential electrolysis of a dichloromethane solution containing $[Mo_2O_2(R_2dtc)_4]PF_6$ at a potential of −0.5 V vs Ag/AgCl proceeded with the passage of 1.1 ± 0.1 faraday/mol at a platinum electrode. In the case of R = ethyl, the resulting purple solution was shown by electrochemistry and UV spectroscopy to contain mainly the well-known species $Mo^{IV}O(Et_2dtc)_2$.[12,19] $MoO(R_2dtc)_2$ can in turn be oxidized at +0.6 V vs Ag/AgCl to regenerate $[Mo_2O_2(R_2dtc)_4]PF_6$ under conditions of controlled-potential oxidative electrolysis with the passage of 0.50 ± 0.05 faraday/mol. These studies were hampered by the fact that $MoO(R_2dtc)_2$ compounds are extremely oxygen sensitive[19] with the ultimate product of aerobic oxidation being $Mo^{VI}O_2(R_2dtc)_2$. Small amounts of the latter were thus detected electrochemically[13] after each electrolysis step. Nevertheless, the reduction (eq 1) and oxidation (eq 2) cycle for the newly isolated $[Mo_2O_2(R_2dtc)_4]^+$ complex cation can be defined.

$$[Mo_2O_2(R_2dtc)_4]^+ + e^- \rightarrow 2MoO(R_2dtc)_2 \quad \text{(ca. −0.35 V vs Ag/AgCl)} \quad (1)$$

$$MoO(R_2dtc)_2 \rightarrow [MoO(R_2dtc)_2]^+ + e^- \quad \text{(+0.6 V vs Ag/AgCl)} \quad (2a)$$

$$MoO(R_2dtc)_2 + [MoO(R_2dtc)_2]^+ \rightarrow [Mo_2O_2(R_2dtc)_4]^+ \quad (2b)$$

De Hayes et al.[12] studied the oxidation of $Mo^{IV}O(Et_2dtc)_2$ in acetonitrile at platinum electrodes. They reported an oxidation process at +0.52 V vs Ag/AgCl under conditions of cyclic voltammetry with a reduction process at −0.26 V vs Ag/AgCl on the reverse scan. While the product of oxidation of $MoO(Et_2dtc)_2$ was not specified by De Hayes et al., it is now clear that it was $[Mo_2O_2(Et_2dtc)_4]^+$.

The only other reported formally mixed oxidation state dimeric complex is $[Mo_2O(R_2dtc)_6]X$ (R = Me, Et; X = BF_4, PF_6, ClO_4).[20] For the ethyl derivative (tetrafluoroborate salt) a structural determination was undertaken and results showed distorted-pentagonal-bipyramidal coordination about each molybdenum center with a bridging oxygen atom. The unpaired electron was effectively delocalized over both metal atoms, and no EPR signal was observed. In the present case, crystals suitable for X-ray structure determination have yet to be prepared. Infrared data (Table IV) provide evidence for the type of bonding involved. Assignments of vibrational modes to infrared bands has been made with reference to previous work on a variety of oxomolybdenum–dithiocarbamate complexes.[13,21] The observation of two absorption bands for the asymmetric Mo–O–Mo stretching mode indicates nonequivalent molybdenum centers, one of which is bonded to a terminal oxygen atom with a resultant absorption at 930–940 cm^{-1} (ν(Mo=O)). The EPR signal for a dichloromethane solution of $[Mo_2O_2(Me_2dtc)_4]PF_6$ shows a major signal (g = 1.98) with a line width of 5 G and hyperfine coupling (A = 37 G) to the molybdenum(V) nuclei ($I = {}^5/_2$). The EPR spectrum is typical of molybdenum(V) species.[10,22-24] The observation of a second signal (g = 1.97, line width = 14 G) at higher concentrations tallies with the electrochemical data concerning the two reduction peaks for $[Mo_2O_2(R_2dtc)_4]PF_6$. Thus the EPR data is also consistent with the postulate that this species aggregates significantly in dichloromethane solution.

II is a structural representation for the $[Mo_2O_2(R_2dtc)_4]^+$ cation consistent with these results. Coordination about the molybdenum(V) atom should be octahedral by comparison with the known structure (III) of the molybdenum(V) dimer $Mo_2O_3(R_2dtc)_4$[25].

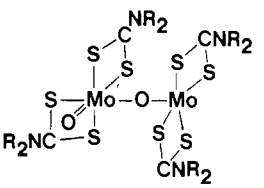

II

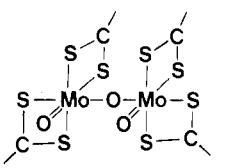

III

The molybdenum(IV) moiety of the mixed-valence complex could be expected to mimic the known series of complexes $MoO(R_2dtc)_2$ with a square-pyramidal arrangement about the metal atom. Therefore while all previously reported dimeric oxomolybdenum complexes have been structurally symmetrical about the bridging atom(s), we propose a compound possessing discrete metal centers of differing oxidation states.

(19) Jowitt, R N.; Mitchell, P. C. H. *J. Chem. Soc. A* **1969**, 2632.
(20) Broomhead, J. A.; Sterns, M.; Young, C. G. *Inorg. Chem.* **1984**, *23*, 729.
(21) Newton, W. E.; Corbin, J. L.; Bravard, D. C.; Searles, J. E. McDonald, J. W. *Inorg. Chem.* **1974**, *13*, 1100.
(22) Swedo, K. B.; Enemark, J. H. *J. Chem. Educ.* **1979**, *56*, 70.
(23) (a) Pickett, C.; Kumar, S.; Vella, P. A.; Zubieta, J. *Inorg. Chem.* **1982**, *21*, 908. (b) Farchione, F.; Hanson, G. R.; Rodrigues, C. G.; Bailey, T. D.; Bagchi, R. N.; Bond, A. M.; Pilbrow, J. R.; Wedd, A. G. *J. Am. Chem. Soc.* **1986**, *108*, 831.
(24) (a) Chou, C. Y.; Huffman, J. C.; Maatta, E. A. *Inorg. Chem.* **1986**, *25*, 822. (b) Chaudhury, M. *Polyhedron* **1986**, *5*, 387.
(25) Ricard, L.; Estienne, J.; Karagiannidis, P.; Toledano, P.; Fischer, J.; Mitschier, A.; Weiss, R. *J. Coord. Chem.* **1974**, *3*, 277.

In accordance with the electrochemical and synthetic data, an equation for the oxidation process at platinum electrodes can be written

$$3MoO(S_2)(R_2dtc)_2 \rightarrow [Mo_2O_2(R_2dtc)_4]^+ + 6S + \text{"MoO"} + [R_4bitt]^{2+} + 3e^- \quad (3)$$

where $[R_4bitt]^{2+}$ represents the 3,5-bis(*N*,*N*-dialkyliminio)-1,2,4-trithiolane 1,2,4 dication that is formed by oxidation of $[R_2dtc]^-$ or R_4tds.[26] The production of another molybdenum-containing species (designated "MoO") during oxidation was verified by demonstrating that along with sulfur, such a species was deposited onto the platinum working electrode during electrolysis. Treatment of the electrode with concentrated nitric acid followed by dilution with water allowed polarographic detection of the compound at the required concentration as molybdate.[27] As written, (3) accounts for 1 faraday/mol of complex. However, further oxidation processes of the kind

$$2\text{"MoO"} + H_2O \rightarrow Mo_2O_3 + 2H^+ + 2e^- \quad (4)$$

or

$$\text{"MoO"} + H_2O \rightarrow MoO_2 + 2H^+ + 2e^- \quad (5)$$

where H_2O is adventitious water, would account for the additional charge associated with the *n* value of 1.5 ± 0.2 faraday/mol. The exact nature of "MoO" adsorbed onto the electrode is unknown. The formation of molybdate on dissolution in nitric acid is expected for a wide range of known oxo- and hydroxymolybdenum compounds. Thus, the seven-coordinate $MoO(S_2)(R_2dtc)_2$ complexes provide an example of a very unusual oxidation process in which reduction in the metal oxidation states occurs by virtue of the presence of readily oxidizable ligands and internal redox processes. The intermediates on the voltammetric time scale are unknown.

(ii) Oxidation Processes for $MoO(S_2)(R_2dtc)_2$ at Mercury Electrodes. The oxidative dc (direct current) polarogram for a dichloromethane solution of $MoO(S_2)(Me_2dtc)_2$ exhibits a complex adsorption-controlled process at considerably less positive potentials than at a platinum electrode. The cyclic voltammogram at a mercury electrode also shows complex behavior and qualitatively resembles the response for a solution of elemental sulfur under the same conditions. As in the case of oxidation at platinum electrodes, the data at mercury electrodes (see Table II) indicate ligand-based electrochemical oxidation involving, in this case, mercury compound formation.

Oxidative controlled-potential electrolysis of $MoO(S_2)(R_2dtc)_2$ in dichloromethane at a mercury pool electrode at 0.75 V vs Ag/AgCl yields a yellow solution showing voltammetric behavior at platinum electrodes identical with that previously described. That is, the soluble products of electrolysis are the same as those produced at a platinum electrode. However, the charge passed during electrolysis is well in excess of the 1.5 faraday/mol recorded at platinum, and a large quantity of an insoluble black powder (oxides/sulfides of mercury) is generated. Thus despite the different mechanism at mercury electrodes, the final product isolated is the same as that found with controlled-potential electrolysis experiments at platinum electrodes.

(iii) Oxidation Processes for $WO(S_2)(Et_2dtc)_2$ and $WS(S_2)(R_2dtc)_2$ at Platinum and Mercury Electrodes. Electrochemical data for the oxidation of these complexes are summarized in Table II. The mode of oxidation at both platinum (Figure 2a) and mercury electrodes appears similar to that for the molybdenum complexes. The oxidation potentials are virtually unaltered by a change from a molybdenum to a tungsten complex. A reduction wave, which is seen on the reverse scan (Figure 2a), as was the case with the molybdenum analogues, is metal and ligand dependent. Oxidative controlled-potential electrolysis ($E_{applied}$ = 1.1 V) resulted in yellow to green solutions. However, the charge passed is in the range of 2–3 faraday/mol and is considerably greater than in the case of molybdenum. Figure 2b shows the cyclic voltammetric response for a solution of $WS(S_2)(Pyrrdtc)_2$ after electrolysis at a platinum electrode. A reduction process is observed at around 0.0 V vs Ag/AgCl (cf. −0.35 V for molybdenum) with a corresponding oxidation wave at 1.1 V vs Ag/AgCl on the reverse scan.

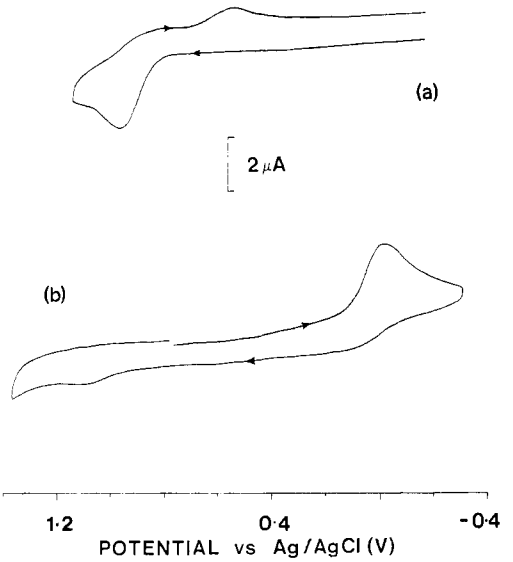

Figure 2. Cyclic voltammograms at a platinum electrode for 2.5×10^{-4} M $WS(S_2)(Pyrrdtc)_2$: (a) oxidative scan; (b) reductive scan after oxidative controlled-potential electrolysis at platinum (+1.1 V). CH_2Cl_2 solutions were used (0.1 M Bu_4NClO_4) at 20 °C (scan rate = 500 mV s^{-1}).

Treatment of $WS(S_2)(Pyrrdtc)_2$ with $NOPF_6$, under nitrogen, yielded a green solution displaying the same behavior as the electrolyzed solutions, but attempts at isolation of the product led to a range of uncharacterized products. That is, $[W_2S_2(R_2dtc)_4]^+$, $[W_2O_2(R_2dtc)_4]^+$, and $[W_2OS(R_2dtc)_4]^+$ are believed to be initially present in electrochemically or chemically oxidized solution, but they are not as stable as $[Mo_2O_2(R_2dtc)_4]^+$.

(iv) Mechanism for Oxidation. The peak potential for oxidation at platinum electrodes (Table II) is not markedly affected by the metal atom or dithiocarbamate R group or whether oxygen or sulfur is bound to the metal. This combined with the strong evidence of the involvement of sulfur in electrochemical responses at mercury electrodes suggests that initially the disulfide (S_2^{2-}) ligand is the site of oxidation. Disulfide oxidation liberates elemental sulfur and facilitates an internal redox process that results in reduction of the metal center and oxidation of the dithiocarbamate ligand. Reactions involving internal electron transfer have been reported recently by Harmer et al.[10] for molybdenum/tungsten–sulfur systems. These authors noted that the redox reactivity of Mo–S systems is quite varied, indicating facile electron transfer between ligand and metal. In the present case the complexes $WS(S_2)(R_2dtc)_2$ and $WO(S_2)(Et_2dtc)_2$ undergo ligand-based oxidation, similar to their molybdenum analogues.

Reduction Studies. (a) Reduction Processes for $MoO(S_2)(R_2dtc)_2$. (i) Mercury Electrodes. Figure 3a shows the polarogram for the reduction of $MoO(S_2)(Et_2dtc)_2$ in dichloromethane. One wave with a half-wave potential of about −1.0 V vs Ag/AgCl is seen for all molybdenum complexes, and dithiocarbamate substituent effects are small (see Table V). In acetone or acetonitrile, the superior negative potential range available reveals a second wave at −1.8 V vs Ag/AgCl. The cyclic voltammogram in Figure 3b at a mercury electrode shows a reduction process at −1.0 V vs Ag/AgCl partially masked by an adsorption-based process at slightly more negative potentials. Comparison with the cyclic voltammogram for a solution of elemental sulfur under the same conditions (Figure 3c) shows a strong resemblance, and as in the case of oxidation, the sulfur present exerts a significant effect on the electrochemical behavior at mercury electrodes. Second and subsequent scans in cyclic voltammetry (Figure 3b) reveal the generation of two processes after

(26) Labuda, J.; Mocak, J.; Bustin, D. I. *Chem. Zvesti*, **1982**, *36*, 633.
(27) Heyrovsky, J.; Zuman, P. *Practical Polarography*; Academic: London, 1968; p 194.

Table V. Voltammetric Data for the Reduction Processes of $MX(S_2)(R_2dtc)_2$ Complexes (M = Mo, X = O; M = W, X = O, S) in Dichloromethane (0.1 M Bu_4NClO_4) at 20 °C

	Pt electrode			Hg electrode cyclic voltammetry[c]		
	cyclic voltammetry[a]		polarography[b]			
compd[d]	E_p^{red}, V	E_p^{ox},[e,h] V	$E_{1/2}$,[h] V	E_p^{red},[h] V	$E_p^{ox}(1)$,[f,h] V	$E_p^{ox}(2)$,[g,h] V
$MoO(S_2)(Me_2dtc)_2$	−1.01	0.07	−1.01	−1.15	−0.58	−0.19
$MoO(S_2)(Et_2dtc)_2$	−1.04	0.06	−1.03	−1.16	−0.58	−0.18
$MoO(S_2)(Bz_2dtc)_2$	−1.05	0.18	−1.03	−1.13	−0.57	−0.15
$MoO(S_2)(c\text{-}Hx_2dtc)_2$	−1.17	−0.01	−1.02	−1.12	−0.65	−0.18
$MoO(S_2)(Pyrrdtc)_2$	−1.04	0.16	−1.00	−1.14	−0.59	−0.16
$WS(S_2)(Bz_2dtc)_2$	−1.04	0.19	−0.65[i]	−1.12	−0.47	−0.21
$WS(S_2)(Pyrrdtc)_2$	−1.05	0.16	−0.66[i]	−1.13	−0.55	−0.10
$WO(S_2)(Et_2dtc)_2$	−1.48	0.07	−1.18	−1.12	−0.59	−0.19
sulfur	−0.96		−1.10	−1.18		−0.14

[a] Platinum disk electrode, scan rate = 500 mV s^{-1}. [b] Dropping mercury electrode, t = 0.5 s. [c] Slowly growing dropping mercury electrode, scan rate = 500 mV s^{-1}. [d] Solution concentration = 1.0×10^{-4} M. [e] Corresponds to the oxidation of released dithiocarbamate ligand; see eq 8. [f] Corresponds to oxidation of electrode mercury in the presence of released dithiocarbamate ligand; see eq 7. [g] Corresponds to oxidation of electrode mercury in the presence of released sulfide. [h] Potential vs Ag/AgCl (saturated LiCl–CH_3CH_2OH). $E_{1/2}[(C_5H_5)_2Fe/(C_5H_5)_2Fe^+]$ = 0.500 V vs Ag/AgCl (saturated LiCl–CH_3CH_2OH). [i] Average value for two poorly resolved waves.

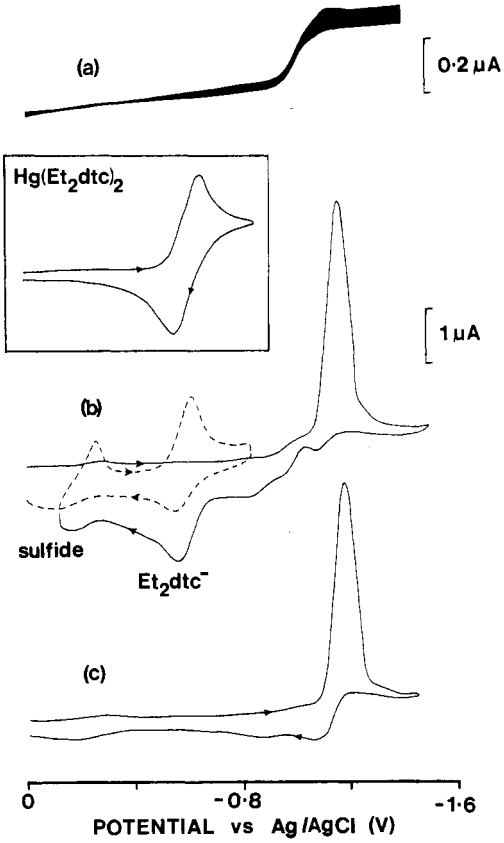

Figure 3. Voltammograms at a slowly growing dropping mercury electrode for the reduction of 1×10^{-4} M complexes: (a) $MoO(S_2)(Et_2dtc)_2$, dc polarogram (drop time 0.5 s); (b) $MoO(S_2)(Et_2dtc)_2$, cyclic voltammogram (scan rate = 500 mV s^{-1}; (—) first scan, (- -) second scan); (c) sulfur, cyclic voltammogram (scan rate = 500 mV s^{-1}). The inset shows a cyclic voltammogram for 2×10^{-4} M $Hg(Et_2dtc)_2$ (scan rate = 500 mV s^{-1}). All solutions are CH_2Cl_2 (0.1 M Bu_4NClO_4) at 20 °C.

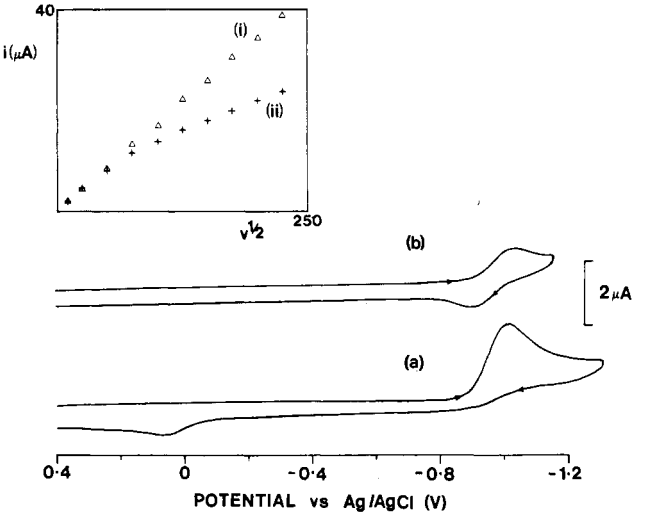

Figure 4. Cyclic voltammograms at a platinum electrode for the reduction of 1×10^{-4} M $MoO(S_2)(Et_2dtc)_2$ in CH_2Cl_2 (0.1 M Bu_4NClO_4) at (a) −70 °C and (b) 20 °C, (scan rate = 500 mV s^{-1}). The inset shows plots of peak current (i, cyclic voltammetry at platinum) versus the square root of scan rate ($v^{1/2}$) for 2.5×10^{-4} M (i) $[(C_5H_5)_2Fe]$ and (ii) $MoO(S_2)(Et_2dtc)_2$ in CH_2Cl_2 (0.1 M Bu_4NClO_4) at 20 °C.

the initial reduction process. The process at −0.6 V vs Ag/AgCl is due to the $Et_2dtc^-/Hg(Et_2dtc)_2$ couple (verified by addition of $Hg(Et_2dtc)_2$). This process arises from the release of diethyldithiocarbamate after reduction of $MoO(S_2)(Et_2dtc)_2$ and corresponds to eq 6. These reactions have been studied in detail[28]

$$2Et_2dtc^- + Hg \rightleftarrows Hg(Et_2dtc)_2 + 2e^- \quad (6)$$

and are believed to involve a Hg(I) intermediate. The other process at more positive potentials is due to the liberation from the reduced molybdenum complex of a species that is formally sulfide, S^{2-}. This process can be seen at the same potential in a cyclic voltammogram after reduction of sulfur (Figure 3c). Electrolysis of a solution of sulfur at a potential more negative than the main process at −1 V results in the passage of 2 faradays/mol and a species that gives a reversible oxidation process at −0.2 V. Thus available evidence indicates that both the dithiocarbamate and sulfur (sulfide) are liberated during the reduction process.

For the molybdenum complexes, reductive controlled-potential electrolysis at a mercury pool electrode in the limiting current region of the DC polarogram (−1.2 V) initially occurs rapidly to yield a brown solution with the passage of 2 faradays/mol. However the current does not fall to zero, and a small residual current still flows. The electrochemistry of the resulting solution confirms the presence of sulfide along with the products of the breakdown of $(Bu_4N)(R_2dtc)$, which is unstable in dichloromethane on the time scale of controlled-potential electrolysis. In addition, very poorly defined reduction processes are seen near the solvent reduction limit, none of which could be identified. When the solvent is changed to either acetone or acetonitrile the electrolysis is complete after transfer of two electrons. The complete stability of $(Bu_4N)(R_2dtc)$ in these solvents suggests that in dichloromethane it is the products of degradation of R_2dtc^- which generate reducible species and prolong electrolysis. Quantification of the electrolysis products was therefore possible

(28) Bond, A. M.; Colton, R.; Dillon, M. L.; Moir, J. E.; Page, D. R. *Inorg. Chem.* **1984**, *23*, 2883.

in acetone and acetonitrile by direct calibration against authentic standards, and results showed the liberation of 1 mol each of sulfide and dithiocarbamate per mole of reduced complex.

(ii) Platinum Electrodes. Figure 4a shows the cyclic voltammogram for a dichloromethane solution of $MoO(S_2)(Et_2dtc)_2$ at a platinum disk electrode. A well-defined chemically irreversible reduction process is observed at −1.0 V vs Ag/AgCl. The reduction potential is similar to the reduction potential observed at mercury electrodes. As with reduction at mercury electrodes there is little variation in reduction potential on varying the dithiocarbamate ligand (Table V). A second peak, also chemically irreversible, is again seen at very negative potentials in acetone or acetonitrile. As shown in Figure 4a, the first reduction process liberates dithiocarbamate as evidenced by the appearance of an oxidation peak on the reverse (oxidative) scan at around 0 V vs Ag/AgCl[26] corresponding to the process

$$2R_2dtc^- \rightarrow R_4tds + 2e^- \quad (7)$$

Comparison of the limiting current per unit concentration for voltammograms obtained at a rotating platinum disk electrode and other metal dithiocarbamates such as $Hg(Et_2dtc)_2$ shows that the reduction at platinum is a two-electron process on the voltammetric time scale as is the case at mercury electrodes.

In Figure 4b the cyclic voltammetric reduction response for $MoO(S_2)(Et_2dtc)_2$ in dichloromethane at −70 °C is shown. A well-defined reversible response is now seen with no evidence of dithiocarbamate being released. Careful exclusion of oxygen from the solution is necessary to achieve this result; otherwise, a poorly defined chemically irreversible response is obtained. The immediate product of the reduction is apparently quite stable at low temperatures in the absence of oxygen since at lower scan rates (50 mV s^{-1}) the ratio of reduction and oxidation currents is close to unity. Experiments with a rotating platinum disk electrode show that at low temperature the reduction process now involves transfer of one electron per molybdenum atom rather than two electrons. Therefore the initial reduction step can be formulated as in (8). Confirmation that the formation of the formally

$$MoO(S_2)(R_2dtc)_2 + e^- \rightleftarrows [MoO(S_2)(R_2dtc)_2]^- \quad (8)$$

molybdenum(V) anion also takes place at room temperatures was obtained by recording cyclic voltammograms at platinum for a range of compounds at scan rates up to 50 V s^{-1}. At fast scan rates the reduction approaches a one-electron process. The data at variable scan rate were evaluated as shown in Figure 4 by plotting the reduction current (i) against the square root of scan rate ($v^{1/2}$). For the one-electron oxidation of ferrocene, a straight line is obtained over the entire range of scan rates (Figure 4). In contrast, the data for reduction of $MoO(S_2)(Et_2dtc)_2$ deviate from linearity as the n value changes from $n = 2$ to $n = 1$.

As in the case of mercury electrodes, controlled-potential electrolysis in the limiting current region of the reduction process (−1.2 V) leads to brown solutions with the passage of 2 faraday/mol of molybdenum complex. The electrochemical behavior following electrolysis is the same as for mercury with sulfide and dithiocarbamate being the only identifiable species in solution. A purple color suggestive of the formation of $Mo^{IV}O(Et_2dtc)_2$ was noted during the course of reductive electrolysis of $MoO(S_2)(Et_2dtc)_2$.

Since 1 mol each of dithiocarbamate and sulfide are liberated at room temperature per mole of complex then the final product(s) appears to have a lowered coordination number as observed in other reduction studies on related compounds.[8,29,30] The extreme sensitivity of monomeric molybdenum(V) intermediates toward disproportionation/dimerization is well-known,[23] with such reactions often catalyzed by traces of water. The extremely high reactivity of the $[MoO(S_2)(R_2dtc)_2]^-$ anion is therefore not unexpected. Additionally compounds of molybdenum(IV) are often air sensitive[19] and may also react with solvents such as chloroform.[31]

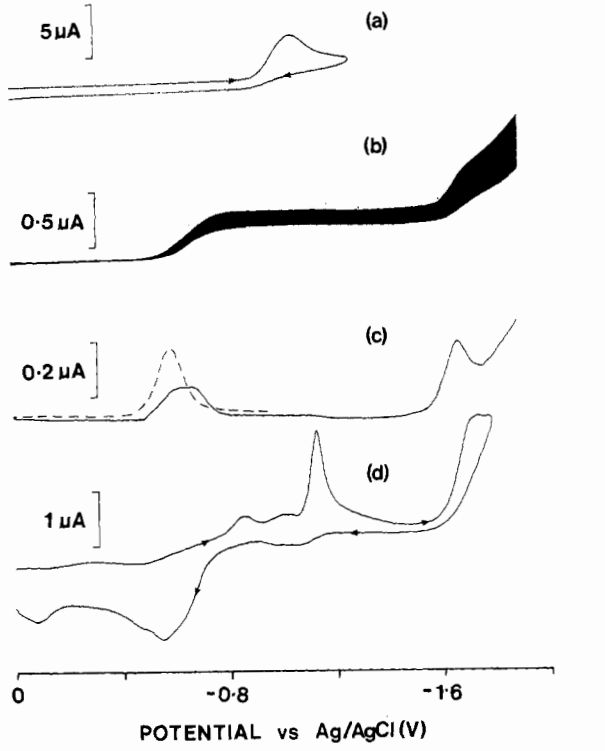

Figure 5. Voltammograms for the reduction of 2.5×10^{-4} M $WS(S_2)(Pyrrdtc)_2$ in CH_2Cl_2 (0.1 M Bu_4NClO_4) at 20 °C: (a) cyclic voltammogram at platinum (scan rate = 500 mV s^{-1}); (b) dc polarogram (drop time 0.5 s); (c) differential-pulse polarogram (drop time 0.5 s, pulse amplitude 50 mV; dotted line corresponds to the response for 2.5×10^{-4} M $Hg(Pyrrdtc)_2$); (d) cyclic voltammogram at mercury (scan rate = 500 mV s^{-1}).

(b) Reduction Processes for $WX(S_2)(R_2dtc)_2$. As well as comparing the influence of changing the metal from molybdenum to tungsten, it is possible to study the effect of replacing the terminal oxygen atom with sulfur while retaining the same metal center. Such a study could not be conducted with molybdenum due to the fact that the complexes $MoS(S_2)(R_2dtc)_2$ are unknown. Attempted synthesis using $Mo(CO)_3(R_2dtc)_2$ a starting material yielded mainly $MoO(S_2)(R_2dtc)_2$.[5] Similarly Harmer et al.[10] have shown that while reaction of WS_4^{2-} with R_4tds yields $WS(S_2)(R_2dtc)_2$, the analogous reaction utilizing MoS_4^{2-} yields $Mo(S_2)(R_2dtc)_3$, a stable, monomeric complex of molybdenum(V). However with tungsten, complexes containing either terminal oxygen or sulfur are available and their reduction properties can be examined.

(i) Reduction Processes for $WO(S_2)(Et_2dtc)_2$ at Platinum and Mercury Electrodes. The cyclic voltammetry at platinum electrodes (Table V) is similar to that of the molybdenum analogue $MoO(S_2)(Et_2dtc)_2$ previously discussed except that reduction occurs at more negative potentials. The shift of −0.4 V in replacing molybdenum with tungsten is as expected for metal-based reduction processes.[9,10] Liberation of free diethyldithiocarbamate is apparent, and the limiting current per unit concentration from rotating disk voltammetry shows that this is a two-electron step. However, the reduction response at a platinum electrode does not become reversible at either low temperature or fast scan rate. This suggests a much greater kinetic and thermodynamic reactivity of the tungsten(V) anion $[WO(S_2)(Et_2dtc)_2]^-$ compared to that of the corresponding molybdenum species $[MoO(S_2)(Et_2dtc)_2]^-$. The reduction process at a mercury electrode is also a two-electron step but occurs at a less negative potential than at a platinum electrode.

(ii) Reduction Processes for $WS(S_2)(R_2dtc)_2$ at Platinum and Mercury Electrodes. Figure 5a shows the voltammetric response

(29) Bradbury, J. R.; Schultz, F. A. *Inorg. Chem.* **1986**, *25*, 4408.
(30) Bradbury, J. R.; Schultz, F. A. *Inorg. Chem.* **1986**, *25*, 4416.
(31) Jasim, K. S.; Chieh, C.; Mak, T. C. W. *Inorg Chim. Acta* **1986**, *116*, 37.

for a solution of $WS(S_2)(Pyrrdtc)_2$ (Pyrrdtc = pyrrolidine-*N*-carbodithioate) in dichloromethane at a platinum electrode. Data in Table V demonstrate that $WS(S_2)(R_2dtc)_2$ complexes are reduced at potentials around 0.4 V less negative than those for $WO(S_2)(Et_2dtc)_2$. This effect is consistent with that observed for similar molybdenum complexes.[12,32] Interestingly this effect also essentially nullifies the negative potential shift that occurred when molybdenum was replaced with tungsten (vide supra). An oxidation response for released dithiocarbamate is also noted, and a second chemically irreversible process near the solvent reduction limit is now seen in dichloromethane as well as in acetone or acetonitrile. Comparison of limiting currents from rotating disk voltammetry with those for known compounds indicates that the tungsten complexes undergo a two-electron-reduction process. The second process at very negative potentials is therefore defined as a one-electron process. At −70 °C reversible behavior is apparent, and a plot of peak current versus the square root of scan rate for $WS(S_2)(Pyrrdtc)_2$ shows a change from a two-electron to a one-electron process as the scan rate is increased. Therefore the complexes $WS(S_2)(R_2dtc)_2$ are also reduced via a tungsten(V) intermediate, and eq 9 is applicable. In contrast no evidence for

$$WS(S_2)(R_2dtc)_2 + e^- \rightleftarrows [WS(S_2)(R_2dtc)_2]^- \quad (9)$$

the existence of $[WO(S_2)(Et_2dtc)_2]^-$ was obtained. Replacement of oxygen by sulfur therefore leads to greater kinetic and thermodynamic stability of the anionic intermediate.

At mercury electrodes there are some marked differences between the behavior of the molybdenum and tungsten complexes. The dc polarogram (Figure 5b) and differential-pulse polarogram (Figure 5c) for $WS(S_2)(Pyrrdtc)_2$ each consists of a two-component response ($E_{1/2}(1) = -0.6$ V, $E_{1/2}(2) = -0.7$ V) with a second, one-electron-reduction wave as observed at platinum electrodes.

The cyclic voltammogram (Figure 5d) shows the reduction process at around −0.6 V followed by a dominant adsorption-based process at around −1.1 V vs Ag/AgCl (due to sulfur). Two processes, (due to $Pyrrdtc^-$ and sulfide), are observed when the potential is switched at very negative potentials, as in the case of the $Hg(R_2dtc)_2/R_2dtc^-$ couple coincides with that of the first wave for $WS(S_2)(R_2dtc)_2$ complexes. This indicates a much stronger and very specific interaction occurs between the tungsten complex and the electrode as has been noted in the reduction of $Cr(R_2dtc)_3$ complexes.[33]

Controlled-potential electrolysis at either a platinum (−1.2 V) or a mercury (−0.8 V) electrode again occurs with the passage of 2 faradays/mol of complex. However in contrast with the molybdenum complexes, a stable electroactive reduction product is formed. The dc polarogram after electrolysis in acetone shows a broad oxidative response at −0.6 to −0.8 V vs Ag/AgCl, which is a two-component chemically reversible wave as was the case with the original reduction response at mercury. The less negative component corresponds to the oxidation of dithiocarbamate released during electrolysis while the second occurs at the same potential as the original reduction response, though with only about half the limiting current. Thus the first reduction process yields a species that is formally $WS(S_2)(R_2dtc)$ according to eq 10a and 10b. The second process, eq 11, corresponds to the reduction

$$2W^{VI}S(S_2)(R_2dtc)_2 + Hg \rightleftarrows 2W^{V}S(S_2)(R_2dtc) + Hg(R_2dtc)_2 \quad (10a)$$

$$Hg(R_2dtc)_2 + 2e^- \rightleftarrows Hg + 2R_2dtc^- \quad (10b)$$

of $W^{V}S(S_2)(R_2dtc)$, without liberation of sulfide. The product of this second reduction can also be produced by the reaction of $WS(S_2)(Pyrrdtc)_2$ with cobaltocene, $CoCp_2$, in oxygen-free dichloromethane. A maroon solid is isolated in low yield, and its electrochemical behavior is identical with that of solutions of $WS(S_2)(Pyrrdtc)_2$ after reductive electrolysis.

This second reduction step is therefore formulated according to eq 11. The $[WS(S_2)(R_2dtc)]^-$ anion is thus the ultimate

$$W^{V}S(S_2)(R_2dtc) + e^- \rightleftarrows [W^{IV}S(S_2)(R_2dtc)]^- \quad (11)$$

product of reductive electrolysis at either platinum or mercury or of chemical reduction with cobaltocene. Reduction is substantially easier at mercury electrodes indicating that specific interaction between the one-electron-reduction product (eq 10a) and electrode mercury provides a lower energy route to $[WS(S_2)(R_2dtc)]^-$. Equations 12 and 13 show a possible scheme for

$$2W^{V}S(S_2)(R_2dtc) + Hg \rightleftarrows Hg[W^{IV}S(S_2)(R_2dtc)]_2 \quad (12)$$

$$Hg[W^{IV}S(S_2)(R_2dtc)]_2 + 2e^- \rightleftarrows Hg + 2[W^{IV}S(S_2)(R_2dtc)]^- \quad (13)$$

reduction at mercury. Thus the series of tungsten complexes $WS(S_2)(R_2dtc)_2$ yield different products, compared to their molybdenum analogues, on the synthetic time scale while showing virtually identical electrochemical behavior at low temperature and in short time scale experiments.

Acknowledgment. We are grateful to Dr. Tony Wedd for recording EPR spectra. We also acknowledge financial support from the Australian Research Grants Scheme.

Registry No. $MoO(S_2)(Me_2dtc)_2$, 71393-29-8; $MoO(S_2)(Et_2dtc)_2$, 64525-55-9; $MoO(S_2)(Bz_2dtc)_2$, 112219-44-0; $MoO(S_2)(c\text{-}Hx_2dtc)_2$, 112196-39-1; $MoO(S_2)(Pyrrdtc)_2$, 112196-40-4; $WS(S_2)(Bz_2dtc)_2$, 112196-41-5; $WS(S_2)(Pyrrdtc)_2$, 108556-17-8; $WO(S_2)(Et_2dtc)_2$, 64525-55-9; S, 7704-34-9; $[Mo_2O_2(Me_2dtc)_4]PF_6$, 112196-43-7; $[Mo_2O_2(Et_2dtc)_4]PF_6$, 112196-45-9; Bu_4NPF_6, 3109-63-5; $NaMe_2dtc$, 128-04-1; Hg, 7439-97-6; Pt, 7440-06-4; Mo, 7439-98-7; W, 7440-33-7; $NOPF_6$, 16921-91-8; $CoCp_2$, 1277-43-6.

(32) Schultz, F. A.; Ott, V. R.; Rolison, D. S.; Bravard, D. C.; McDonald, J. W.; Newton, W. E. *Inorg. Chem.* **1978**, *17*, 1758.
(33) Bond, A M.; Wallace, G. G. *Inorg. Chem.* **1984**, *23*, 1858.